Cue-Dependent Fear Learning Drives Nucleus Accumbens Spine Plasticity

Desh Deepak Ratna[1], Cortez Gray[3], Eugene Lee[1], Harris Kiaris[3], Makenna Hamilton[3], T. Chase Francis[1,2]*

Affiliations

1) Department of Psychiatry, University of Maryland, School of Medicine, Baltimore, Maryland 21201, USA
2) UM-MIND, University of Maryland, Baltimore, Baltimore, Maryland 21201, USA
3) Department of Drug Discovery and Biomedical Sciences, College of Pharmacy, University of South Carolina, Columbia, South Carolina 29208, USA

*Correspondence: chase.francis@som.umaryland.edu

Keywords: Plasticity, Spine morphology, Synaptic Plasticity, AMPA receptor, Substance P, Fear Conditioning

Abstract

Nucleus accumbens (NAc) dopamine 2 receptor expressing medium spiny neurons (D2-MSNs) are involved in stress and aversive learning, where repeated stress increases excitatory spine density. Whether this plasticity reflects cue-specific learning or generalized stress response remains unknown. Using Pavlovian fear conditioning in Tac1-Cre/Tdtomato mice, we dissociated associative plasticity from the effects of foot shock stress. Acute fear conditioning produced distinct physiological outcomes between stress in the presence or absence of a cue. Conditioning for 7 days consolidated cue learning and increased excitatory transmission frequency via an increase in the total spine density. However, repeated exposure to foot shock did not lead to this synaptic remodeling. Our results suggest that morphological changes supporting synaptic plasticity on NAc D2-MSNs are due to cue-dependent learning, but not foot shock stress alone. We propose that NAc D2-MSNs encode learning and response to threat cues, which may heighten later stress responsivity.

Introduction

Stress-related brain areas detect and encode environmental cues based on their valence and salience, which helps organisms distinguish between safe and threatening conditions, and is required for survival. Acute stress is adaptive and can mobilize energy reserves for a reactive response and enhance aversive learning to threatening stimuli [1-3]. However, prolonged stress exposure causes maladaptive alterations in neuronal structure and signaling [4,5], resulting in pathological conditions including depression and anxiety [6,7]. However, the number and duration of stressors required to induce these structural and physiological changes, as well as the intersection between learning and negative emotional outcomes, have not been thoroughly explored.

The Nucleus Accumbens (NAc) has recently been identified as a key locus necessary for the expression of stress and aversive responses [8,9]. NAc medium spiny projection neurons (MSNs), characterized by their dopamine 1 (D1) or dopamine 2 (D2) receptor expression, play distinct roles in processing aversive stimuli, where D1-MSNs are required for cue-dependent aversive conditioning, and D2-MSNs are necessary for cue-dependent recall [10-12]. In addition, D2-MSNs have been implicated in learning in other contexts, including negative reinforcement [13,14], decision-making [12,15], reversal learning [16,17], and reward learning [12,14]. These studies indicate that D2-MSNs play a more subtle role in aversive response and may not directly contribute to negative outcomes to stress.

NAc MSN subtypes display dichotomous excitatory synaptic changes following repeated stress. Interestingly, despite depression-related outcomes being attributed to decreased NAc function [8,18,19], repeated stress increases the density of excitatory spines on D2-MSNs and increases the frequency of excitatory input [8,9,20,21]. Whereas in D1-MSNs, structural changes after repeated stress reduce excitatory transmission and D1-MSN activity bidirectionally alters depression-related outcomes [5,8,22-25] . Further evidence indicates that activating D2-MSNs during an acute, mild social stressor promotes social avoidance without affecting hedonic outcomes [8], and spine density correlates with social avoidance [21]. Regardless of the animal's stress-susceptibility state, these observations suggest that D2-MSNs facilitate a learned or generalized avoidance response towards a stressor or aversive stimuli, helping identify harmful environmental cues. This study aims to determine how NAc D2-MSN morphological plasticity confers specific cued features about stressful stimuli.

In this study, we tested the hypothesis that plasticity in NAc D2-MSNs is driven by conditioned aversive cues rather than by repeated non-conditioned foot shock. Pavlovian fear conditioning was used to assess aversive learning and to provide a repeated foot shock stressor. Surprisingly, we found plasticity on NAc D2-MSNs shifted across repeated foot shock from an increase in amplitude to an increase in the frequency of excitatory synaptic input. Our study further provided proof of principle by testing how substance P-dependent signaling, which is necessary for NAc D2-MSN plasticity and cue-dependent learning, blunts this plasticity and learning through an unexpected decrease in

release probability. Our data underscores the importance of NAc D2-MSN excitatory plasticity in learning about aversive stimuli and diminishes the role of D2-MSNs in stress-related outcomes.

Material and methods

Animals

All animal experimental protocols followed in this study were approved by the Institutional Animal Care and Use Committee of the University of South Carolina and the University of Maryland, Baltimore. Both female and male mice were used in the study, and all mice were maintained in a facility with a 12:12 reverse light-dark cycle (lights off at 7:00; lights on at 19:00) and provided with ad libitum access to food and water. All the behavior experiments were performed during the active period of mice. Mice breeders were procured from Jackson Laboratory, and breeding colonies were maintained in the university animal facility. Tac1-IRES2-Cre mice (Jackson Laboratory strain 021877) were bred with tdTomato (Ai14, Jackson Laboratory strain 007914) reporter mice, generating Tac1-Cre/tdTomato reporter mouse line. To confirm the presence of Tac1-Cre and tdTomato allele, ear punch tissue samples were used for genotyping. Weaning was done at postnatal day 21, and same-sex housing groups were maintained. The colonies were housed in a climate-controlled facility.

Pavlovian fear conditioning

Fear conditioning (FC) was conducted in sound-attenuating fear conditioning chambers (Med Associates, USA). Prior to each conditioning session, mice were habituated in a separate room for 30 min under the same lighting conditions used for that session (training or cue-recall). All the experimental mice were assigned to one of the four conditioning procedures: (a) Paired conditioning, Conditioned stimulus (CS+) paired with an unconditioned stimulus (US+) (CS+US+); (b) Tone only, CS+ with no unconditioned stimulus (US-) (CS+US-); (c) Shock only (US+), with no conditioned stimulus (CS-) (CS-US+); (d) Context only (CS-US-). Conditioning was conducted in context A for 1, 3, 5, or 7 days, during which mice were placed in a chamber with an exposed metal grid, white light, and a vanilla scent (10% vanilla extract in ethanol). Following a 2 min baseline, mice in the paired conditioning group (CS+US+) received a 10 sec white-noise cues (80 dB), which co-terminated with a 0.6 mA foot shock, separated by a 30 sec interval. Mice received two pairings each day. Control groups receive only the tone (CS+US-), shock (CS-US+), or context only (CS-US-). Post-conditioning, after 24 hrs, mice were placed in a new context (context B) to test cue recall, in which 5 white noise cues that did not produce extinction were provided at 30 sec intervals after a 2 min baseline. Context B contained a chamber with an opaque white plexiglass floor insert, a curved wall insert, near-infrared (NIR) light, and vinegar scent (1% acetic acid in water). Freezing behavior during conditioning and recall was analyzed and used as a metric for

87 learned aversive behavior. Brains were collected immediately after the cue recall for whole-cell patch-clamp
88 electrophysiology.
89
90 ***Slice electrophysiology***
91 Whole-cell electrophysiological recordings were performed on the cue recall day. Brains were extracted after
92 brief 3% isoflurane anesthesia and cervical dislocation. 300 μm sections were cut on a vibratome (Leica VT1000S) in
93 ice-cold N-Methyl D-Glucamine (NMDG) cutting artificial cerebrospinal fluid (ACSF) solution (in mM): 92 NMDG, 20
94 HEPES, 25 glucose, 30 sodium bicarbonate, 1.2 sodium phosphate, 2.5 potassium chloride, 5 sodium ascorbate, 3
95 sodium pyruvate, 2 thiourea, 10 magnesium, 0.5 calcium chloride, osmolarity 305–310 mOsm, pH 7.34. Immediately
96 after slicing, slices were placed in warm (32 ºC) NMDG solution for 2–5 min, then transferred to HEPES holding solution
97 at room temperature for 1 h, which was the same as NMDG solution except NMDG was replaced with 92 mM sodium
98 chloride and contained 1 mM magnesium chloride and 2 mM calcium chloride. Recording was performed at 33ºC, and
99 slices were washed at a rate of 2 mL/min with ACSF (in mM): 125 sodium chloride, 26 sodium bicarbonate, and 11
100 glucose, 2.5 potassium chloride, 1.25 sodium phosphate, 2.4 calcium chloride, 1 magnesium chloride, osmolarity 305–
101 310 mOsm, pH 7.34. To block inhibitory currents, synaptic recordings were performed by holding cells at -70 mV in the
102 presence of picrotoxin (100 μM) added to the ACSF. Cesium methanesulfate with neurobiotin (0.1%) was used as the
103 internal solution (in mM): 117 cesium methanesulfonate, 20 HEPES, 2.8 sodium chloride, 4 magnesium ATP, 0.3 sodium
104 GTP, 0.4 EGTA, pH 7.30, osmolarity 280–287 mOsm.
105 Whole-cell recordings were obtained in the NAc core using borosilicate glass pipettes (1.5-3.0 MΩ). D2-MSNs
106 were distinguished from D1-MSNs by the absence of Tdtomato fluorescence using an Olympus BX51WI microscope
107 and an LED light source (Olympus). After giga-seal formation and breaking in the cell, cells were allowed to stabilize
108 for 5 min before data acquisition. Signals were amplified using a Multiclamp 700B amplifier and digitized (Digidata
109 1550B, Molecular Devices) at a 10 kHz sampling rate and filtered at 1 kHz for spontaneous excitatory postsynaptic
110 currents (sEPSCs) and 2-4 kHz for electrically evoked currents. Synaptic currents were evoked using a concentric
111 bipolar stimulating electrode. AMPAR/NMDAR ratios were acquired by taking the peak of the inward current at -70 mV
112 divided by the +40 mV outward current 50 msec after the start of the AMPAR response. Paired pulse ratios (PPRs)
113 were acquired at a 50 msec interval and were calculated as response 2/response 1. All evoked currents were the
114 average of at least 7 sweeps. Cells with <20MΩ series resistance were included in the analysis and cells showing 20%
115 or greater change in series resistance were excluded from analysis. Following recording, slices were collected in a 4%
116 paraformaldehyde solution in 1X PBS for 24hrs before being placed in 1X PBS solution in 0.01% sodium azide for
117 processing.

118 ***Neuronal morphology***

119 Neurons filled with neurobiotin were processed for neuronal morphology assessment. PFA-fixed slices in
120 0.01% sodium azide were washed in 1X PBS three times for 30 min each. Sections were then incubated in a blocking
121 solution of 1X PBS with 0.5% Triton X-100 (20%), 10% Normal Donkey Serum (NDS) for 5 hrs at room temperature.
122 Slices were then incubated overnight at room temperature in 1:1000 Steptavadin-488 (Jackson Laboratory, cat#016-
123 540-084) in a modified blocking solution with 0.05% Triton X-100 (20%) and 10% NDS in 1XP BS. To remove unbound
124 Streptavidin-488, slices were washed 3 times in 1X PBS for 30 minutes each. Slices were placed in 1X PBS, carefully
125 mounted, dried, and cover-slipped using DAPI mounting medium. All images were acquired using a Leica TCS SP8
126 multiphoton confocal microscopy system (Leica Microsystems, Germany) and LASX software (Leica Microsystems,
127 Germany). The images were captured at 40x-63x magnification using a GFP filter to visualize the streptavidin-488
128 tagged neurobiotin-filled neuron. Secondary dendrites were identified and imaged using Leica's z-stack function to
129 maintain a 3-D information of spines (see **Supplemental Figure 3**).

130 Spines were quantified using ImageJ. Secondary dendrites 10-30 μm in length and perpendicular to the beam
131 path were chosen for quantification. Spines were quantified in each plane of the z-stack without using a z-stack
132 projection. Spine types (Mushroom, Stubby, and Thin) were empirically determined using previous and current hand-
133 scored datasets, which quantified head size and neck length and identified spine types by eye. Spine types were
134 assigned using the following parameters: spine head area (μm^2), neck length (μm)): Mushroom (≥0.2, >0.2); Stubby
135 (>0.2, <0.2); Thin (<0.2, >0.2).

136

137 ***Statistical analysis***

138 Detailed statistics are provided in **Supplementary Table 1**. The reported data were analyzed, and statistics
139 were calculated using GraphPad Prism software, and significance was considered if $P<0.05$. For all multi-group data,
140 two-way ANOVAs were used followed by post-hoc tests using Tukey's multiple comparison test. Student's *t*-test was
141 used only for the L-733,060 and saline injection groups in the 7-day CS+US+ condition. All data are represented as the
142 mean ± SEM.

143

144 **Results**

145 ***Repeated fear conditioning increases cue-dependent learning***.

146 Our previous work and others have indicated that NAc D2-MSN activation facilitates social avoidance learning,
147 but not depression-related outcomes and D2-MSN activity is driven by increased spine density [8,26]. To determine if
148 repeated conditioning produces the same D2-MSN effects as repeated social stress, Tac1-Cre/tdTomato mice were

149 subjected to a Pavlovian fear conditioning protocol and underwent 1, 3, 5, and 7 days of conditioning (**Fig. 1a**). Following
150 1-day conditioning, freezing was tested in a novel context to determine the extent to which mice associated the cue
151 with the aversive foot shock. As we have shown previously [10], two pairings of conditioned stimulus (CS) paired with an
152 unconditioned stimulus (US) foot shock (CS+US+), led to significant freezing, compared to unpaired groups (CS-US-,
153 CS-US+, CS+US-) (**Fig. 1b**), confirming cue-dependent learning. In addition, mice showed an enhancement in freezing
154 to the cue as well as the conditioning context. After 7 days of repeated conditioning, freezing during recall was higher
155 in the CS+US+ group than other groups (**Fig. 1c**). Baseline freezing was similar across all groups, with moderate
156 freezing observed in the US+ condition for both CS- and CS+ groups, consistent with stress sensitization or context
157 generalization [27,28]. As expected, repeated conditioning days augmented freezing to both the context and the tone (**Fig.**
158 **1d**).
159
160 ***Repeated fear conditioning alters synaptic inputs.***
161 To understand the underlying synaptic changes in D2-MSNs involved in the cue-dependent learning for
162 aversive cues, we performed whole-cell patch clamp recordings from D2-MSNs (**Fig. 2**). Following a single day of
163 conditioning, spontaneous excitatory postsynaptic current (sEPSC) amplitude was increased in D2-MSNs in the
164 CS+/US+ group (**Fig. 2a**), as shown previously [10]. sEPSC frequency, AMPAR/NMDAR ratios, and PPR showed no
165 change across all other conditions (**Fig. 2a-b**). In the 3- and 5-day conditioning groups, no differences were observed
166 (**Supplementary Fig. 1**). In contrast, 7-day conditioning animals revealed a selective increase in frequency in the
167 CS+US+ group compared to the CS-US- group, with no change in CS conditions (**Fig. 2c**). These higher rates of
168 spontaneous excitatory events, accompanied by no change in amplitude, AMPAR/NMDAR ratios, or PPR (**Fig. 2c-d**),
169 and in the rectification **(Supplementary Fig. 2)**, implicating a shift in plasticity that may underlie long-term learning.
170
171 ***Repeated conditioning shifts plasticity by increasing the number of spines.***
172 Increased sEPSC frequency, without a change in PPR, indicates increased excitatory connectivity onto D2-
173 MSNs which could be mediated by an increase in spine density. To directly test whether this is due to structural synaptic
174 remodeling and link it to freezing behavior, dendritic spine density and morphology were quantified in the same recorded
175 neurons (**Fig. 3; Supplementary Fig. 3**). After one day of conditioning, no differences were observed in spine density
176 (**Fig 3a-b**). However, after 7 days of repeated conditioning, the total spine density was significantly increased in
177 CS+US+ group compared to all other groups (**Fig. 3c-d**). Furthermore, classification of spine subtypes shows an
178 increase in thin and mushroom spines in the CS+US+ group [29], and no change in stubby spines (**Fig. 3d**). These results

179 suggest spine formation supports the long-term cue-dependent learning observed in 7-day freezing and may underlie
180 the increase in frequency of excitatory transmission.
181
182 ***Blocking substance P signaling reduces release probability.***
183 The striatum has dense expression of the primary receptor for substance P, the neurokinin 1 receptor (NK1R)
184 [30], and activation of the NK1R promotes selective excitatory plasticity on NAc D2-MSNs [31]. Our previous work has
185 shown that NAc substance P signaling is required for cue-dependent aversive learning from one day of fear conditioning
186 [10]. In addition, systemic and local antagonism or NAc knockout of the NK1R prior to one day conditioning prevents
187 enhanced synaptic strength on D2-MSNs [10,30]. Therefore, we tested whether repeated antagonism of the NK1R could
188 block physiological changes caused by repeated conditioning. L-733,060 selectively increased PPR without affecting
189 sEPSC amplitude or frequency (**Fig. 4a-b**) or AMPAR/NMDAR ratios (**Fig. 4c**), indicating reduced presynaptic release
190 probability. This suggests an unknown and putatively active mechanism to blunt fear memories, caused by antagonism
191 of the NK1R.
192
193 **Discussion**
194 In this study, our data verify our previous results that NAc D2-MSN plasticity is caused by cue-dependent
195 conditioning [10] and extends this dataset to show that repeated conditioning leads to significant and, sustained changes
196 in plasticity through an increase in spine density. Furthermore, our data indicates that conditioned cues are required for
197 this plasticity, not just foot shock alone, and this plasticity can be blunted by additional mechanisms to reduce excitatory
198 transmission on NAc D2-MSNs. These results provide evidence that learned aversive stimuli, not just the aversive,
199 stressful stimuli alone, promote D2-MSN plasticity. Previous studies have shown that repeated stress increases the
200 density of excitatory spines on D2-MSNs [21]. Electrophysiological measures recorded from 7 days CS+US+ conditioning
201 mice showed that the postsynaptic excitatory input on NAc D2-MSNs is increased via an increase in excitatory spine
202 density sEPSCs. This outcome is similar, if not equivalent, with earlier studies where mice received chronic stress [8,32].
203 Furthermore, activation of NAc D2-MSNs specifically during an aversive social cue produces enhanced social
204 avoidance without explicitly causing anhedonia [8]. Concurrently, spine alterations, which are an important hallmark of
205 dynamic neuronal plasticity and are important in learning [33], were not observed in cue-independent contextual learning
206 following foot shock only. This supports our idea that structural remodeling at these synapses is associated with the
207 formation of a stabilized fear memory that is cue-selective and not necessarily a generalized response to aversive cues.
208 Together, these data suggest D2-MSN synapses are engaged in cue-dependent fear learning through coordinated
209 structural and functional mechanisms.

Substance P is highly expressed in NAc and acts via NK1R [10,30,31,34], and its signaling is known to be important for learning about aversive cues [12]. Interestingly, mice injected with NK1R antagonist allowed us to delineate learning-related synaptic plasticity from presynaptic modulation in NAc D2-MSNs. We found PPR was selectively increased at D2-MSNs synapses, indicating reduced presynaptic release probability that may compensate for increased frequency of excitatory input on D2-MSNs. We also observed no change in sEPSC amplitude and frequency, further revealing that this manipulation does not affect the exact mechanisms causing an increase in excitation that support learned behavior. These observations show that D2-MSNs fine-tune the circuit dynamics, consistent with a gain-setting modulatory role for substance P [35].

Taken together, our findings support a model (**Fig. 5**) in which fear learning is encoded through specific synaptic modifications on D2-MSNs that dissociate learned threat from generalized stress responses important for cue-dependent aversive response. We propose that the learning component of aversive conditioning is encoded by D2-MSNs and may contribute to how stress responses are perceived and processed.

Acknowledgements

This work was supported by NIH/NIMH R00MH123673, the Department of Drug Discovery and Biomedical Sciences in the College of Pharmacy at the University of South Carolina, and the Department of Psychiatry at the University of Maryland School of Medicine.

Author Contributions

Conceptualization, D.D. and T.C.F.; methodology and investigation, D.D., C.G., E.L., H.K., M.H., and T.C.F.; writing, D.D., C.G., and T.C.F.; review and editing, D.D., E.L., and T.C.F.; supervision, T.C.F.

Data Availability

Data is available upon request from the corresponding author.

Additional Information

The authors declare no competing interests.

References

1 James, P. H. *et al.* Regulation of the hypothalamic-pituitary-adrenocortical stress response. *Compr Physiol* **6**, 603–621, (2016). https://doi.org/10.1002/cphy.c150015

2 Kaileigh, A. B. *et al.* Acute stress enhances tolerance of uncertainty during decision-making. *Cognition* **205** (2020). https://doi.org/10.1016/j.cognition.2020.104448

3 Gjerstad, J. K., Lightman, S. L. & Spiga, F. Role of glucocorticoid negative feedback in the regulation of HPA axis pulsatility. *Stress* **21**, 403–416 (2018). https://doi.org/10.1080/10253890.2018.1470238

4 Ronald, S. D., Gerard, S. & John, H. K. Altered connectivity in depression: GABA and glutamate neurotransmitter deficits and reversal by novel treatments. *Neuron* **102**, 75–90 (2019). https://doi.org/10.1016/j.neuron.2019.03.013

5 Francis, T. C. *et al.* Molecular basis of dendritic atrophy and activity in stress susceptibility. *Mol Psychiatry* **22**, 1512–1519 (2017). https://doi.org/10.1038/mp.2017.178

6 Carlo, F. *et al.* Childhood stressful events, HPA axis and anxiety disorders. *World J Psychiatry* **2**, 13–25 , (2012). https://doi.org/10.5498/wjp.v2.i1.13

7 Sameer, H. Chronic stress, neuroinflammation, and depression: an overview of pathophysiological mechanisms and emerging anti-inflammatories. *Front Psychiatry* **14** (2023). https://doi.org/10.3389/fpsyt.2023.1130989

8 Francis, T. C. *et al.* Nucleus accumbens medium spiny neuron subtypes mediate depression-related outcomes to social defeat stress. *Biol Psychiatry* **77**, 212–222 (2015). https://doi.org/10.1016/j.biopsych.2014.07.021

9 Francis, T. C. & Lobo, M. K. Emerging role for nucleus accumbens medium spiny neuron subtypes in depression. *Biol Psychiatry* **81**, 645–653 (2017). https://doi.org/https://doi.org/10.1016/j.biopsych.2016.09.007

10 Belilos, A. *et al.* Nucleus accumbens local circuit for cue-dependent aversive learning. *Cell Rep* **42**, 113488 (2023). https://doi.org/10.1016/j.celrep.2023.113488

11 Carina, S.-C., Barbara, C., Nuno, S. & Ana, J. R. Reappraising striatal D1- and D2-neurons in reward and aversion. *Neurosci Biobehav Rev* **68**, 370–386 , Elsevier (2016). https://doi.org/10.1016/j.neubiorev.2016.05.021

12 Jennifer, E. Z. *et al.* D1 and D2 medium spiny neurons in the nucleus accumbens core have distinct and valence-independent roles in learning. *Neuron* **112**, 835–849.e837 , (2024). https://doi.org/10.1016/j.neuron.2023.11.023

13 You Hsin, L. *et al.* Accumbal D2R-medium spiny neurons regulate aversive behaviors through PKA-Rap1 pathway. *Neurochem Int* **143** (2021). https://doi.org/10.1016/j.neuint.2020.104935

14 Carina, S.-C. *et al.* Nucleus accumbens medium spiny neurons subtypes signal both reward and aversion. *Mol Psychiatry* **25**, 3241–3255 , Mol Psychiatry (2020). https://doi.org/10.1038/s41380-019-0484-3

15 Elena Chaves, R., Jérémie, N., Daniel, R. & Alban de, K. Direct and indirect striatal projecting neurons exert strategy-dependent effects on decision-making. (2025).

16 Jérôme, L., Alexander, S. J., Colin, M. & Jentsch, J. D. Dopamine D2 receptors in dopaminergic neurons modulate performance in a reversal learning task in mice. *eNeuro* **5** (2018). https://doi.org/10.1523/ENEURO.0229-17.2018

17 Tom, M., Ji Yoon, K. & Takatoshi, H. Nucleus accumbens core dopamine D2 receptor-expressing neurons control reversal learning but not set-shifting in behavioral flexibility in male mice. *Front Neurosci* **16** (2022). https://doi.org/10.3389/fnins.2022.885380

18 Yudan, D. *et al.* Reduced nucleus accumbens functional connectivity in reward network and default mode network in patients with recurrent major depressive disorder. *Transl Psychiatry* **12** (2022). https://doi.org/10.1038/s41398-022-01995-x

19 Bingqian, Z. *et al.* Alterations of static and dynamic functional connectivity of the nucleus accumbens in patients with major depressive disorder. *Frontiers in Psychiatry* **13** (2022). https://doi.org/10.3389/fpsyt.2022.877417

20 Daniel, J. C. *et al.* IκB kinase regulates social defeat stress-induced synaptic and behavioral plasticity. *J Neurosci* **31**, 314–321 (2011). https://doi.org/10.1523/JNEUROSCI.4763-10.2011

21 Megan, E. F., Antonio, F., Miriam, S. M. & Mary Kay, L. Dendritic spine density is increased on nucleus accumbens D2 neurons after chronic social defeat. *Sci. Rep.* **10** (2020). https://doi.org/10.1038/s41598-020-69339-7
22 Francis, T. C., Gaynor, A., Chandra, R., Fox, M. E. & Lobo, M. K. The selective RhoA inhibitor rhosin promotes stress resiliency through enhancing D1-medium spiny neuron plasticity and reducing hyperexcitability. *Biol Psychiatry* **85**, 1001–1010 (2019). https://doi.org/10.1016/j.biopsych.2019.02.007
23 Lucantonio, F. *et al.* Ketamine rescues anhedonia by cell-type- and input-specific adaptations in the nucleus accumbens. *Neuron* **113**, 1398–1412 e1394 (2025). https://doi.org/10.1016/j.neuron.2025.02.021
24 Pignatelli, M. *et al.* Cooperative synaptic and intrinsic plasticity in a disynaptic limbic circuit drive stress-induced anhedonia and passive coping in mice. *Mol Psychiatry* **26**, 1860–1879 (2021). https://doi.org/10.1038/s41380-020-0686-8
25 Lim, B. K., Huang, K. W., Grueter, B. A., Rothwell, P. E. & Malenka, R. C. Anhedonia requires MC4R-mediated synaptic adaptations in nucleus accumbens. *Nature* **487**, 183–189 (2012). https://doi.org/10.1038/nature11160
26 Fox, M. & Lobo, M. The molecular and cellular mechanisms of depression: a focus on reward circuitry. *Mol Psychiatr*, 1–18 (2019). https://doi.org/10.1038/s41380-019-0415-3
27 Arp, J. M. *et al.* Blocking glucocorticoid receptors at adolescent age prevents enhanced freezing between repeated cue-exposures after conditioned fear in adult mice raised under chronic early life stress. *Neurobiol Learn Mem* **133**, 30–38 , (2016). https://doi.org/10.1016/j.nlm.2016.05.009
28 Jiahui, Y., Toshie, N. & Masanori, S. Fear generalization immediately after contextual fear memory consolidation in mice. *Biochem Biophys Res Commun* **558**, 102–106 , (2021). https://doi.org/10.1016/j.bbrc.2021.04.072
29 Kalen, P. B. & Elly, N. Spine dynamics: are they all the same? *Neuron* **96**, 43–55 (2017). https://doi.org/10.1016/j.neuron.2017.08.008
30 Virginia, M. P., Jennifer, D., June, C., Patrick, D. G. & Nigel, W. B. Neurokinin 1 receptor distribution in cholinergic neurons and targets of substance P terminals in the rat nucleus accumbens. *J Comp Neurol* **423**, 500–511 (2000). https://doi.org/10.1002/1096-9861(20000731)423:33.0.CO;2-9
31 Francis, T. C., Yano, H., Demarest, T. G., Shen, H. & Bonci, A. High-frequency activation of nucleus accumbens D1-msns drives excitatory potentiation on D2-msns. *Neuron* **103**, 432–444 e433 (2019). https://doi.org/10.1016/j.neuron.2019.05.031
32 Lena, A. K. *et al.* Stress and Cocaine Trigger Divergent and Cell Type. 2013;Specific Regulation of Synaptic Transmission at Single Spines in Nucleus Accumbens. *Biol Psychiatry* **79**, 898–905 , Elsevier (2016). https://doi.org/10.1016/j.biopsych.2015.05.022
33 Gipson, C. D. & Olive, M. F. Structural and functional plasticity of dendritic spines - root or result of behavior? *Genes Brain Behav* **16**, 101–117 (2017). https://doi.org/10.1111/gbb.12324
34 Toshihiko, A. & Yasuo, K. Actions of substance P on rat neostriatal neurons in vitro. *The Journal of Neuroscience* **16**, 5141–5153 (1996). https://doi.org/10.1523/JNEUROSCI.16-16-05141.1996 ,
35 Zi Xuan, H., Ting Yu, L., Yue Yue, Y., Hui Fang, S. & Xiao Juan, Z. Substance P plays a critical role in synaptic transmission in striatal neurons. *Biochem Biophys Res Commun* **511**, 369–373 , Elsevier B.V. (2019). https://doi.org/10.1016/j.bbrc.2019.02.055

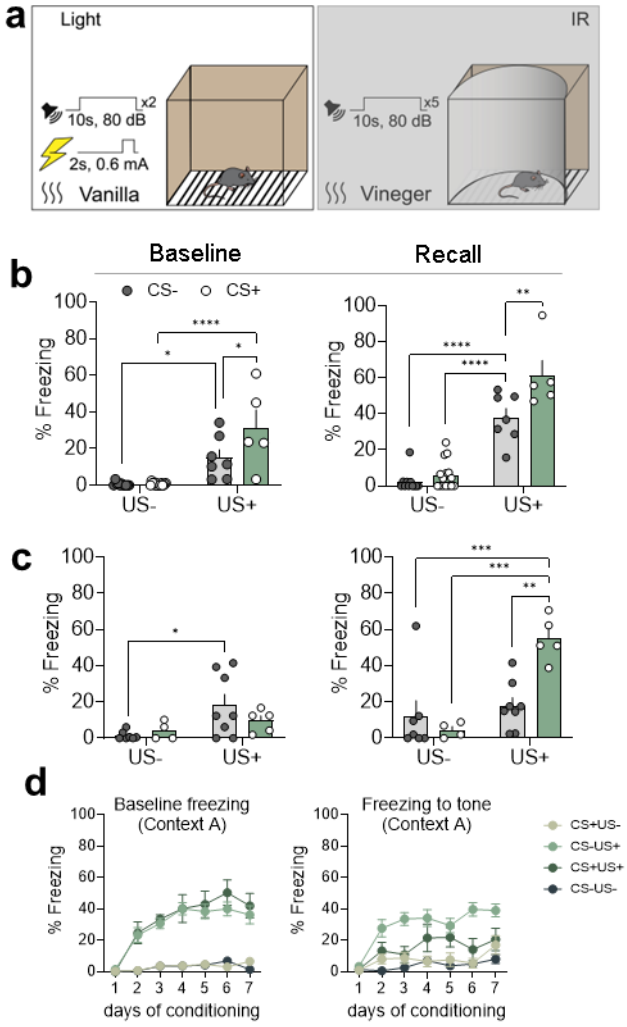

Figure 1. Freezing across a single day or multiple days of fear conditioning. (a) Schematic diagram of the fear conditioning paradigm used for aversive learning. **(b)** Baseline freezing in a novel context (context B) followed by recall in 1-day group. **(c)** Baseline freezing in context B followed by recall in 7-day group. **(d)** 7-day freezing in conditioning context (context A) to the context (*left*) or the cue in context A (*right*). Data are represented as mean± SEM, **P*<0.05, ***P*<0.01, ****P<0.0001,* *****P<0.0001*. For a detailed statistical table, see **Supplementary Table 1**.

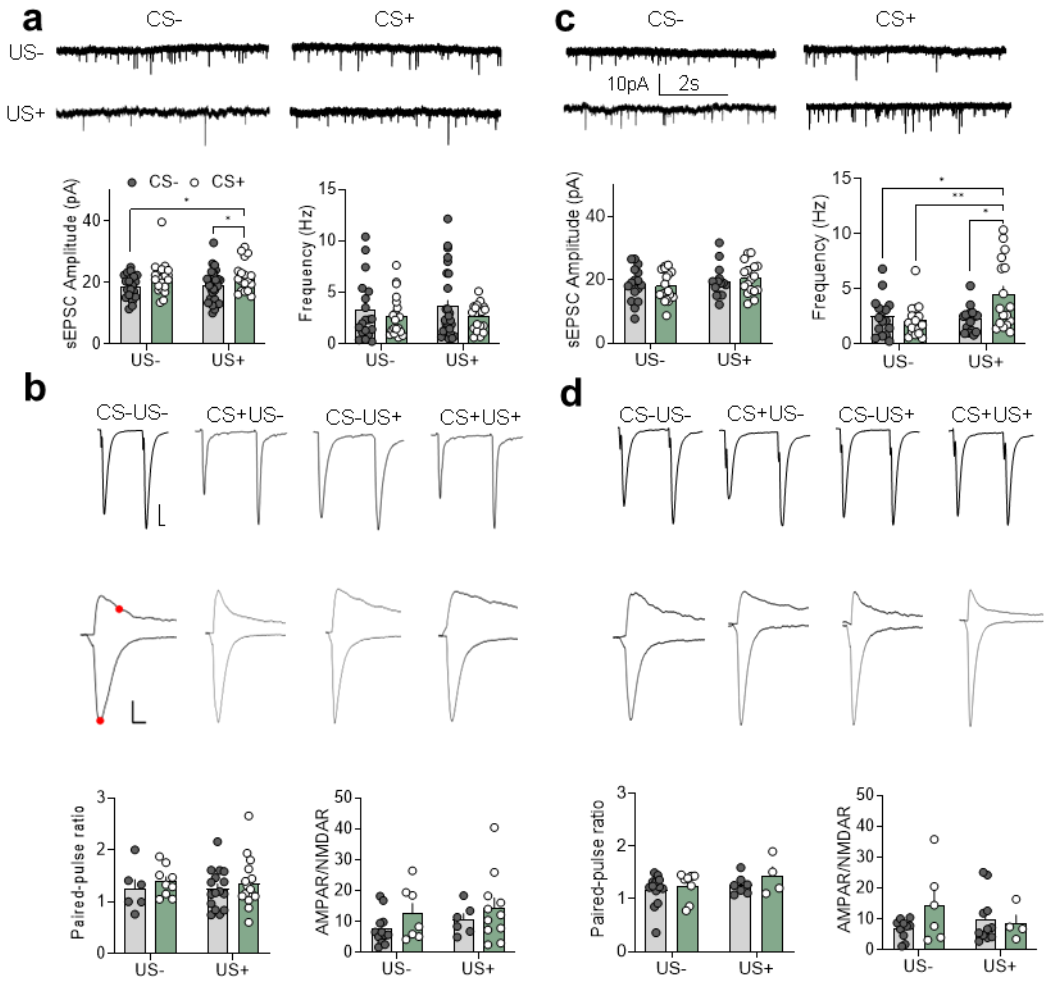

Figure 2. Repeated conditioning promotes increased excitation plasticity on NAc D2-MSNs. sEPSC amplitude and frequency for **(a)** 1-day and **(c)** 7-day groups with representative traces for sEPSCs. PPR and AMPAR/NMDAR for **(b)** 1-day and **(d)** 7-day conditioning group with representative traces for PPR and AMPAR/NMDAR. Red dots indicate the acquisition of AMPAR currents (negative, -70 mV peak) and NMDAR currents (positive, 40 mV amplitude at 50 msec). Data are represented as mean± SEM, *P<0.05, *P<0.01. For a detailed statistical table, see **Supplementary Table 1**.

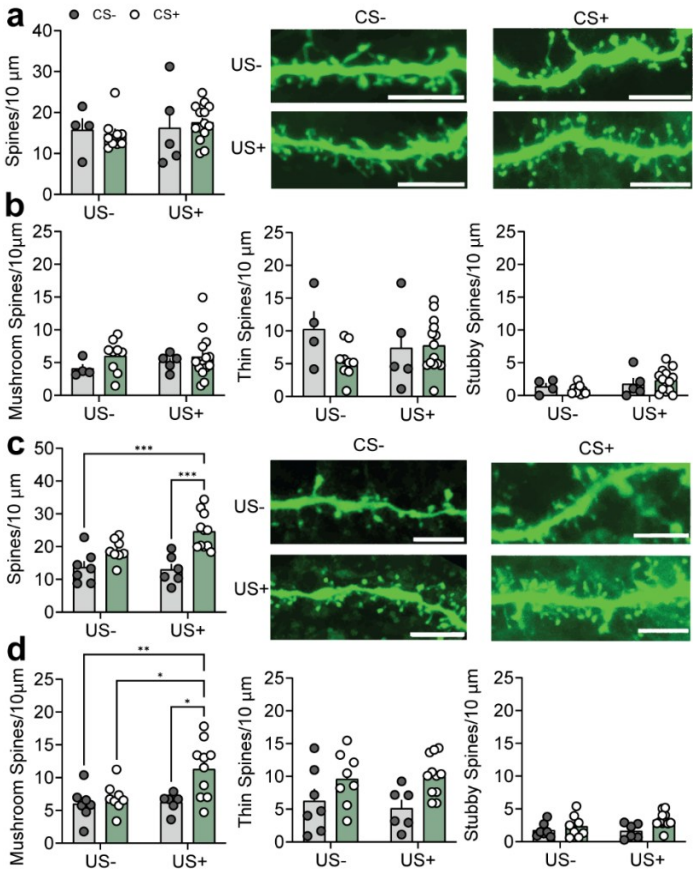

Figure 3. Spine density increases after 7-days of cue-shock conditioning. (a) Total spine density after 1-day fear conditioning and **(b)** mushroom, thin, and stubby spine density. **(c)** 7-day fear conditioning and **(d)** mushroom, thin, and stubby spines density. Scale bar 5 µm. Data are represented as mean± SEM, **P*<0.05, ****P*<0.001, *****P*<0.0001. For a detailed statistical table, see **Supplementary Table 1**.

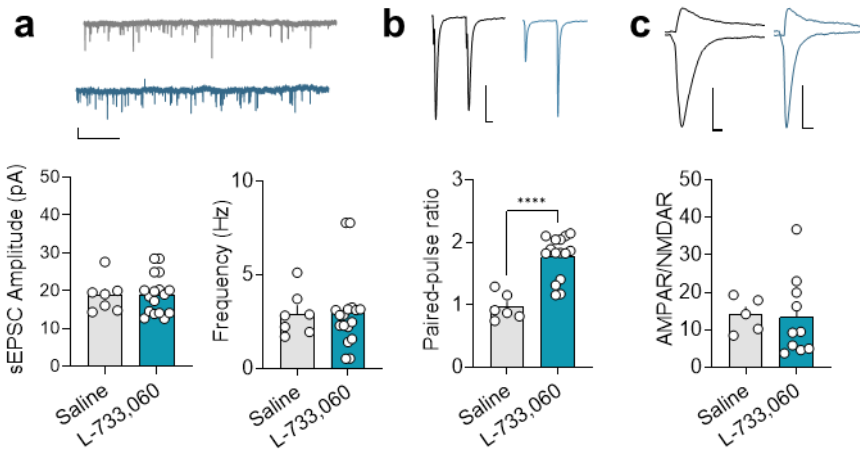

Figure 4. Blocking substance P signaling promotes reduced presynaptic release. **(a)** sEPSCs amplitude and frequency, **(b)** PPR, and **(c)** AMPAR/NMDAR after recall in mice injected with saline or the NK1R antagonist L-733,060 prior to each conditioning day. Upper panels showing representative traces. Data are represented as mean± SEM, **P*<0.05, ****P*<0.001, *****P*<0.0001. For a detailed statistical table, see **Supplementary Table 1**.

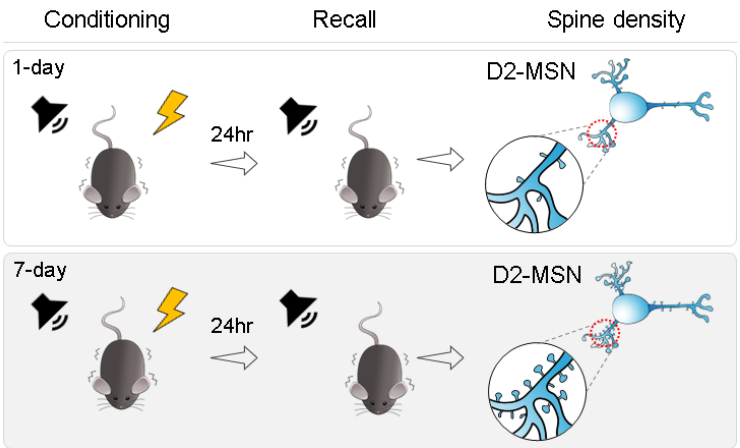

Figure 5. An increase in the total number of spines is encoded by threat learning, not a generalized mechanism, after 7 days of fear conditioning.

Supplementary Figures and Tables

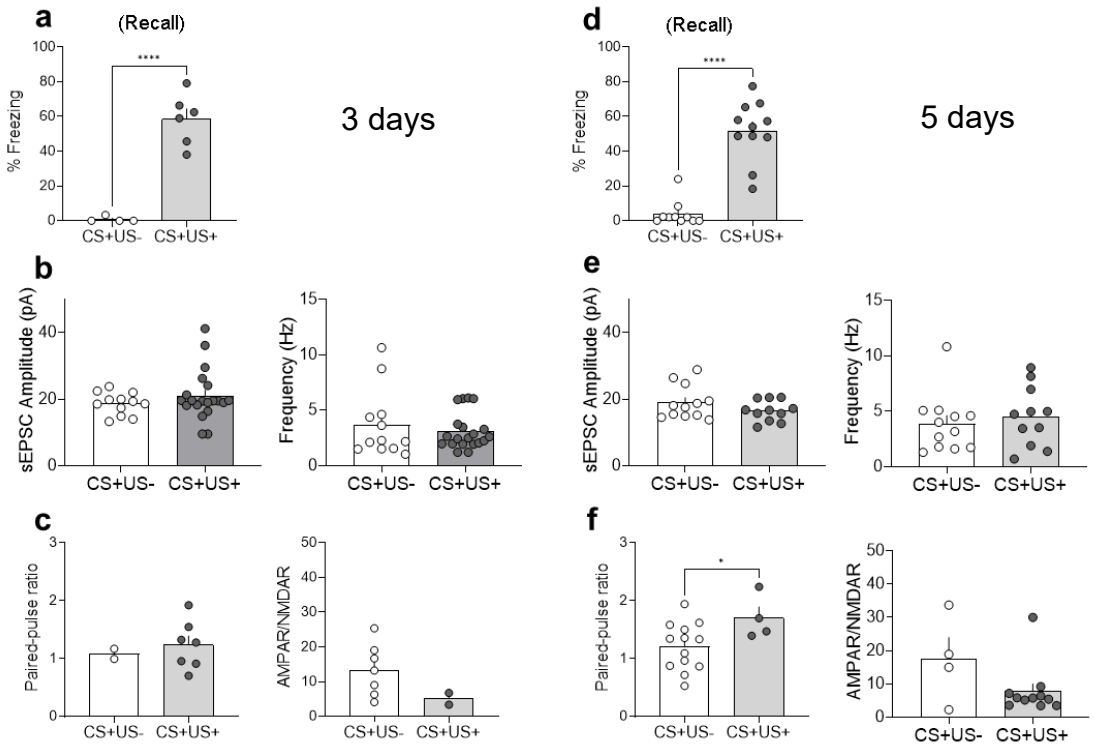

Supplementary Figure 1. Electrophysiological measures are unchanged following 3 or 5 days of conditioning. (a) 3-days of conditioning enhanced freezing to the cue ($t(8) = 7.634$, $P<0.0001$). **(b)** sEPSC amplitude and frequency remained unchanged after 3-days of conditioning. Mice/cells (N/n): CS+US-=4/12, CS+US+=6/20. **(c)** PPR, and AMPAR/NMDAR ratios remained unchanged after 3-days of conditioning. **(d)** 5-days of conditioning enhanced freezing to the cue ($t(19) = 8.087$ $P<0.0001$). N/n: CS+US-=4/2, CS+US+=6/7. **(e)** sEPSCs amplitude and frequency and AMPAR/NMDAR ratios remained unchanged after 5-days of conditioning. N/n: CS+US-=10/12, CS+US+=11/11. **(f)** PPR was changed after 5-days of conditioning ($P<0.0496$, $t(15) = 2.136$) while AMPAR/NMDAR ratios remained unchanged. N/n: CS+US-=10/13, CS+US+=11/4. Data are represented as mean± SEM, *$P<0.05$, ****$P<0.0001$.

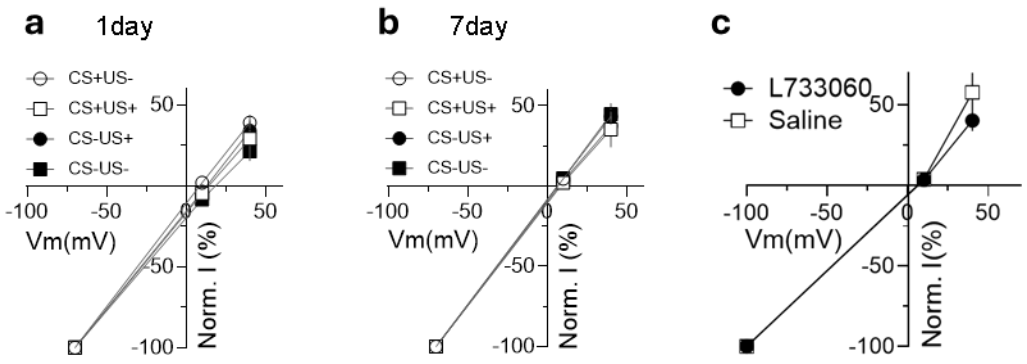

Supplementary Figure 2. AMPAR IVs remain unchanged after fear conditioning. AMPAR-evoked current-voltage relationship remained unchanged after **(a)** 1-day (Two-way RM ANOVA, no interaction, $F(6,82) = 0.4493$, $P = 0.8435$, N/n: CS+US-=5/8, CS+US+= 7/13, CS-US+= 7/16, CS-US-= 3/8) or **(b)** 7-days (Two-way RM ANOVA, no interaction, $F(6,38) = 0.3812$, $P = 0.8864$, N/n: CS+US-= 3/5, CS+US+= 1/2, CS-US+= 5/8, CS-US-= 4/8) of conditioning. **(c)** No change after 7-days of conditioning was observed in AMPAR IV curves in Sal or L-733,060 injected mice (Two-way RM ANOVA, no interaction, $F(2, 18) = 0.0.9482$, $P=0.4059$). N/n: Sal= 5/7, L-733060= 3/4. Data are represented as mean± SEM.

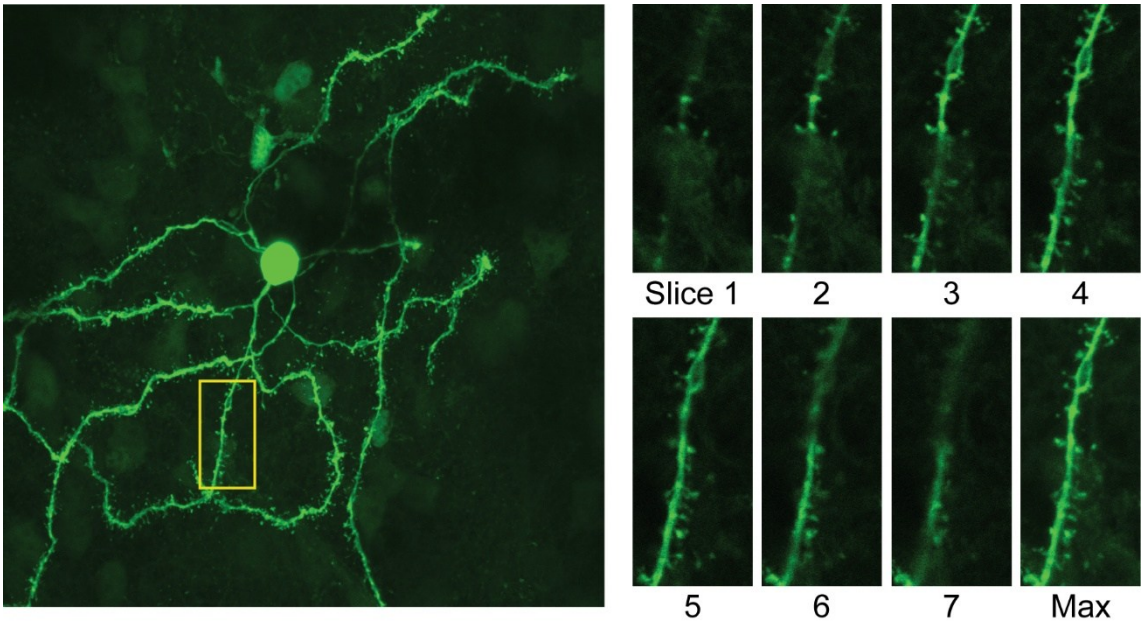

Supplementary Figure 3. Three-dimensional spine analysis. (*left*) Images of dendritic arbors were acquired and secondary dendrites within the plane of the focus were isolated and analyzed. (*right*) An individual secondary spine from the yellow insert. Dendritic spines were quantified using individual z-slices. Three-dimensional images were used to decrease loss of information by a stack maximum (Max).

Supplementary Table 1: Exact Statistics

Fig	Panel	Test	Test Statistic		*P*-value	N
1	(b) Baseline freezing	Two-way ANOVA	CS, US	Interaction $F(1, 34) = 6.281$	0.0172	11,15, 7,5
				Main effect of US, $F(1,34) = 49.01$	0.0001	
				Main effect of CS, $F(1, 34) = 6.408$	0.0162	
			CS-US- vs CS+US-	Tukey's mc $q(34) = 0.0317$	*0.9*	
			CS-US- vs CS-US+	Tukey's mc $q(34) = 4.650$	0.0120	
			CS-US- vs CS+US+	Tukey's mc $q(34) = 8.840$	0.0001	
			CS+US- vs CS-US+	Tukey's mc q(34) =4.884	0.0078	
			CS+US- vs CS+US+	Tukey's mc $q(34) = 9.209$	0.0001	
			CS-US+ vs CS+US+	Tukey's mc $q(34) = 4.303$	0.0222	
	Recall freezing	Two-way ANOVA	CS, US	Interaction $F(1,34) = 6.971$	0.0124	
				Main effect of CS, $F(1,34) = 13.03$	0.0010	
				Main effect of US, $F(1,34) = 148.5$	0.0001	
			CS-US- vs CS-US-	Tukey's mc $q(34) = 1.222$	0.8233	
			CS-US- vs CS-US+	Tukey's mc $q(34) = 9.875$	0.0001	
			CS-US- vs CS+US+	Tukey's mc $q(34) = 14.65$	0.0001	
			CS+US- vs CS-US+	Tukey's mc $q(34) = 9.371$	0.0001	
			CS+US- vs CS+US+	Tukey's mc $q(34) = 14.36$	0.0001	
			CS-US+ vs CS+US+	Tukey's mc $q(34) = 5.339$	0.0033	
	(c) Baseline freezing	Two-way ANOVA	CS, US	No interaction $F(1,20) = 1.469$	0.2396	7,4,8, 5
				Main effect of CS, $F(1,20) = 0.416$	0.5263	
				Main effect of US, $F(1,20) = 5.805$	0.0257	
		Two-way ANOVA	CS, US	Interaction $F(1,20) = 11.45$	0.0029	
				Main effect of CS, $F(1,20) = 4.870$	0.0392	
				Main effect of US, $F(1,20) = 17.74$	0.0004	
			CS-US- vs CS+US-	Tukey's mc $q(20) = 1.125$	0.8556	
			CS-US- vs CS-US+	Tukey's mc $q(20) = 0.98581$	0.9044	
			CS-US- vs CS+US+	Tukey's mc $q(20) = 6.567$	0.0008	
			CS+US- vs CS-US+	Tukey's mc $q(20) = 1.961$	0.5215	
			CS+US- vs CS+US+	Tukey's mc $q(20) = 6.783$	0.0006	
			CS-US+ vs CS+US+	Tukey's mc $q(20) = 5.875$	0.0025	
2	(a) sEPSC amplitude	Two-way ANOVA	CS, US	No interaction $F(1, 82) = 0.014$	0.9055	19,21 ,28, 18
				Main effect of CS, $F(1,82) = 7.304$	0.0084	
				Main effect of US, $F(1,82) = 0.1313$	*0.7181*	

	sEPSC frequency	Two-way ANOVA	CS, US	No interaction $F(1, 82) = 0.1353$ Main effect of CS, $F(1,82) = 1.830$ Main effect of US, $F(1,82) = 0.07$	*0.7139* *0.1798* *0.792*	
	(b) sEPSC amplitude	Two-way ANOVA	CS, US	No interaction $F(1, 60) = 0.3432$ Main effect of CS, $F(1,60) = 0.017$ Main effect of US, $F(1,60) = 1.722$	*0.5602* *0.8942* *0.1944*	16,17,14,17
	sEPSC frequency	Two-way ANOVA	CS, US	Interaction $F(1, 62) = 6.799$ Main effect of CS, $F(1,62) = 3.284$ Main effect of US, $F(1,62) = 4.247$	0.0114 0.0748 0.0435	
			CS-US- vs CS+US-	Tukey's mc test, $q(62)=0.7952$	*0.9428*	
			CS-US- vs CS+US-	Tukey's mc test, $q(62)=0.5384$	*0.9810*	
			CS-US- vs CS+US-	Tukey's mc test, $q(62)=3.873$	*0.0392*	
			CS-US- vs CS+US-	Tukey's mc test, $q(62)=0.2487$	*0.9980*	
			CS-US- vs CS+US-	Tukey's mc test, $q(62)=4.741$	*0.0073*	
			CS-US- vs CS+US-	Tukey's mc test, $q(62)=4.420$	*0.0140*	
	(c)PPR	Two-way ANOVA	CS, US	Interaction $F(1, 44) = 0.018$ Main effect of CS, $F(1,44) = 0.02$ Main effect of US, $F(1,44) = 0.8436$	0.8926 0.3634 0.888	6,9,16,17
	AMPAR/NMDAR	Two-way ANOVA	CS, US	Interaction $F(1, 32) = 0.043$ Main effect of CS, $F(1,32) = 02.421$ Main effect of US, $F(1,32) = 0.7178$	0.8365 0.4032 0.1296	12,7,6,11
	(d) PPR	Two-way ANOVA	CS, US	Interaction $F(1, 28) = 0.1503$ Main effect of CS, $F(1,28) = 1.350$ Main effect of US, $F(1,28) = 1.682$	0.7011 0.2551 0.2052	13,8,7,4
	AMPAR/NMDAR	Two-way ANOVA	CS, US	Interaction $F(1, 27) = 0.2193$ Main effect of CS, $F(1,27) = 1.047$ Main effect of US, $F(1,27) = 0.1896$	0.1502 0.3154 0.6667	10,6,11,4
3	(a)total spines	Two-way ANOVA	CS, US	No interaction $F(1, 28) = 0.2898$ Main effect of CS, $F(1,28) = 0.004$ Main effect of US, $F(1,28) = 0.5737$	0.5946 0.9476 0.4551	4,9,5,14
	Mushroom spines	Two-way ANOVA	CS, US	No interaction $F(1, 28) = 0.2561$ Main effect of CS, $F(1,28) = 1.428$ Main effect of US, $F(1,28) = 0.1580$	0.6168 0.2422 0.6940	
	Thin spines	Two-way ANOVA	CS, US	No interaction $F(1, 28) = 2.408$ Main effect of CS, $F(1,28) = 1.770$ Main effect of US, $F(1,28) = 0.023$	0.1319 0.1941 0.8801	

	Stubby spines	Two-way ANOVA	CS, US	No interaction $F(1, 28) = 0.7226$ Main effect of CS, $F(1,28) = .0007$ Main effect of US, $F(1,28) = 2.413$	0.4025 0.9779 0.1316	
	(c) total spines	Two-way ANOVA	CS, US	No interaction $F(1, 28) = 3.549$ Main effect of CS, $F(1,28) = 24$ Main effect of CS, $F(1,28) = 2.127$	0.070 0.0001 0.1558	7,8,6, 11
	(d) mushroom spines	Two-way ANOVA	CS, US	No interaction $F(1, 27) = 3.442$ Main effect of CS, $F(1, 27) = 7.261$ Main effect of US, $F(1, 27) = 4.238$	0.0745 0.0120 0.0493	
			CS-US- vs CS+US-	Tukey's mc q(28) =0.8384	0.9394	
			CS-US- vs CS+US-	Tukey's mc q(28) =02.1889	0.9991	
			CS-US- vs CS+US+	Tukey's mc q(28) =4.986	0.0078	
			CS-US- vs CS+US	Tukey's mc q(28) =0.6088	0.9727	
			CS+US- vs CS+US+	Tukey's mc q(28) = 4.266	0.0266	
			CS-US+ vs CS+US+	Tukey's mc q(28) =4.555	0.0165	
	Thin spines	Two-way ANOVA	CS, US	No interaction $F(1, 28) = 0.3063$ Main effect of CS, $F(1,28) = 9.010$ Main effect of US, $F(1,28) = 0.6797$	0.5844 0.0056 0.7962	
	Stubby spines	Two-way ANOVA	CS, US	No interaction $F(1, 28) = 1.311$ Main effect of CS, $F(1,28) = 5.624$ Main effect of US, $F(1,28) = 0.7584$	0.2618 0.0248 0.3912	
4	(a) sEPSC amplitude	Two-tailed unpaired *t*-test	Saline vs L-733,060	$t(22)=0.1215$	0.9044	7,17
	sEPSC Frequency	Two-tailed unpaired *t*-test	Saline vs L-733,060	$t(22)=0.0562$	0.9556	
	(b) Paired-pulse ratio	Two-tailed unpaired *t*-test	Saline vs L-733,060	$t(19) = 5.357$	0.0001	6,15
	(c)AMPAR/NMDAR	Two-tailed unpaired *t*-test	Saline vs L-733,060	$t(13) = 0.1229$	0.9041	5,10